A Compact Quad-Band Bandpass Filter Using Multi-Mode Stub-Loaded Resonator

Lakhindar Murmu[*] and Sushrut Das

Abstract—This paper presents a compact shorted stub-loaded quad-band bandpass filter. The proposed filter simultaneously operates at GSM (0.83–0.97 GHz), LTE2300 (2300–2400 MHz), WiMAX (3.3–3.7 GHz), and WLAN (5.725–5.825 GHz) bands. The filter has been designed using the technique of stub-loaded resonator (SLR). By changing the length of the center-loaded stub, the resonant frequency of the even-mode can be varied without affecting that of the odd-mode. This simplifies the design and tuning of the quad-band filter. Eight transmission zeros (TZs) around the three passband make the pass bands highly isolated. In order to validate its practicability, a quad-band bandpass filter (BPF) has been designed, fabricated and measured. Good agreement between simulated and measured results is observed.

1. INTRODUCTION

Recently, due to the rapid development of various wireless communication services, multiband filters have attracted considerable attention as essential components for combination of GSM, LTE, WiMAX and WLAN band applications. Huge amount of research on dual- and triple-passband filter synthesis was presented based on the techniques of loaded stub, frequency transformation and coupling matrix. However, most of these studies consider only the filters with specific passband response [1–5]. A few researches also address the method of generalized design [6, 7]. However, these filters have narrow bandwidth and limited passband and stopband regions. Very few researches on quad-band BPF design have been reported [8–17]. In [8], dual-behavior resonator has been applied to split a wide passband into multiple passbands. However, it is difficult to independently manipulate the frequency response of each passband in this technique. Quad-band bandpass filter with multiple transmission zeros has been reported in [9] utilising symmetrical stub-loaded resonator and even and odd-mode analysis technique. Although it provides one transmission zero and four transmission poles for the four passbands, the isolation between two pass bands is not satisfactory. The quad-band BPF covering 2.4, 3.5, 5.2, and 5.8 GHz has been reported in [10], which applies high-temperature superconducting material to reduce the insertion loss. This filter possesses a few TZs and no sharp skirt between passbands. So it is still meaningful to carry out high-performance quad-band BPFs with compact size, closely spaced passbands, low insertion loss, high return loss and sharp skirt to satisfy the whole WLAN application demands.

Conventional SIRs can shift the higher order resonant mode. Thus some approaches also use the higher order frequencies to create another passband [11–16]. But the conventional SIRs have dual discontinued steps, causing more loss and larger circuit area.

In this paper, a quad-band, stub-loaded resonator with multi-mode characteristic is presented on the basis of previous works [1, 4]. Because of its symmetric structure property, even-odd-mode method is utilized to analyze its resonance characteristics. The position of all the passbands can be predicted based on even-mode and odd-mode analysis using EM full-wave simulations. To get high skirt selectivity,

The authors are with the Department of Electronics Engineering, Indian School of Mines, Dhanbad, India.

the resonator as well as loaded stubs is bent to create transmission zero. In this way, without using either additional stubs or additional lumped elements, it makes the BPF electrically small and easy for fabrication. The quad-band BPF is fabricated and measured using Keysight PNA N5221A network analyzer. Measured results exhibit good agreement with the simulated ones.

2. RESONATOR ANALYSIS

A basic stub loaded resonator, consisting of six open stubs and one shorted stub, is shown in Figure 1(a). For even-mode excitation, there is no current flow through the symmetrical plane, and we can bisect the circuit at the middle to obtain the even mode equivalent circuit of Figure 1(b). The even mode circuit can further be decomposed into four resonant circuits, shown in Figure 1(d). For odd-mode excitation, there exists a voltage null along the middle of the structure, and the therefore, the odd-mode equivalent circuit can be represented as Figure 1(c). As before, it can be decomposed into four resonant circuits, shown in Figure 1(e).

The input admittance (Y) and resonance frequencies (f) of the even- and odd-modes can be expressed as [1]:

$$Y_{\text{in, odd1}} = \frac{Y_1}{j \tan(\theta_1 + \theta_3 + \theta_5 + \theta_7)} \tag{1}$$

$$f_{\text{odd1}} = \frac{(2n-1)c}{4(L_1 + L_3 + L_5 + L_7)\sqrt{\varepsilon_e}} \tag{2}$$

$$Y_{\text{in, even1}} = -jY_1 \frac{Y_S - 2Y_1 \tan(\theta_1 + \theta_3 + \theta_5 + \theta_7)\tan\theta_s}{2Y_1 \tan(\theta_s) + Y_S \tan(\theta_1 + \theta_3 + \theta_5 + \theta_7)} \tag{3}$$

$$f_{\text{even1}} = \frac{(2n-1)c}{4(L_1 + L_3 + L_5 + L_7 + L_s)\sqrt{\varepsilon_e}} \tag{4}$$

$$Y_{\text{in, odd2}} = -jY_2 \frac{Y_1 - Y_2 \tan\theta_2 \tan(\theta_3 + \theta_5 + \theta_7)}{Y_2 \tan(\theta_3 + \theta_5 + \theta_7) + Y_1 \tan\theta_2} \tag{5}$$

$$f_{\text{odd2}} = \frac{(2n-1)c}{4(L_2 + L_3 + L_5 + L_7)\sqrt{\varepsilon_e}} \tag{6}$$

$$Y_{\text{in, even2}} = -jY_2 \frac{Y_1 - Y_2 \tan\theta_2 \tan(\theta_3 + \theta_5 + \theta_7 + \theta_s)}{Y_2 \tan(\theta_3 + \theta_5 + \theta_7 + \theta_s) + Y_1 \tan\theta_2} \tag{7}$$

$$f_{\text{even2}} = \frac{(2n-1)c}{4(L_2 + L_3 + L_5 + L_7 + L_s)\sqrt{\varepsilon_e}} \tag{8}$$

$$Y_{\text{in, odd3}} = -jY_4 \frac{Y_1 - Y_4 \tan\theta_4 \tan(\theta_5 + \theta_7)}{Y_4 \tan(\theta_5 + \theta_7) + Y_1 \tan\theta_4} \tag{9}$$

$$f_{\text{odd3}} = \frac{(2n-1)c}{4(L_4 + L_5 + L_7)\sqrt{\varepsilon_e}} \tag{10}$$

$$Y_{\text{in, even3}} = -jY_4 \frac{Y_1 - Y_4 \tan\theta_4 \tan(\theta_5 + \theta_7 + \theta_s)}{Y_4 \tan(\theta_5 + \theta_7 + \theta_s) + Y_1 \tan\theta_4} \tag{11}$$

$$f_{\text{even3}} = \frac{(2n-1)c}{4(L_4 + L_5 + L_7 + L_s)\sqrt{\varepsilon_e}} \tag{12}$$

$$Y_{\text{in, odd4}} = -jY_6 \frac{Y_1 - Y_6 \tan\theta_6 \tan\theta_7}{Y_6 \tan\theta_7 + Y_1 \tan\theta_6} \tag{13}$$

$$f_{\text{odd4}} = \frac{(2n-1)c}{4(L_6 + L_7)\sqrt{\varepsilon_e}} \tag{14}$$

$$Y_{\text{in, even4}} = -jY_6 \frac{Y_1 - Y_6 \tan\theta_6 \tan(\theta_7 + \theta_s)}{Y_6 \tan(\theta_7 + \theta_s) + Y_1 \tan\theta_6} \tag{15}$$
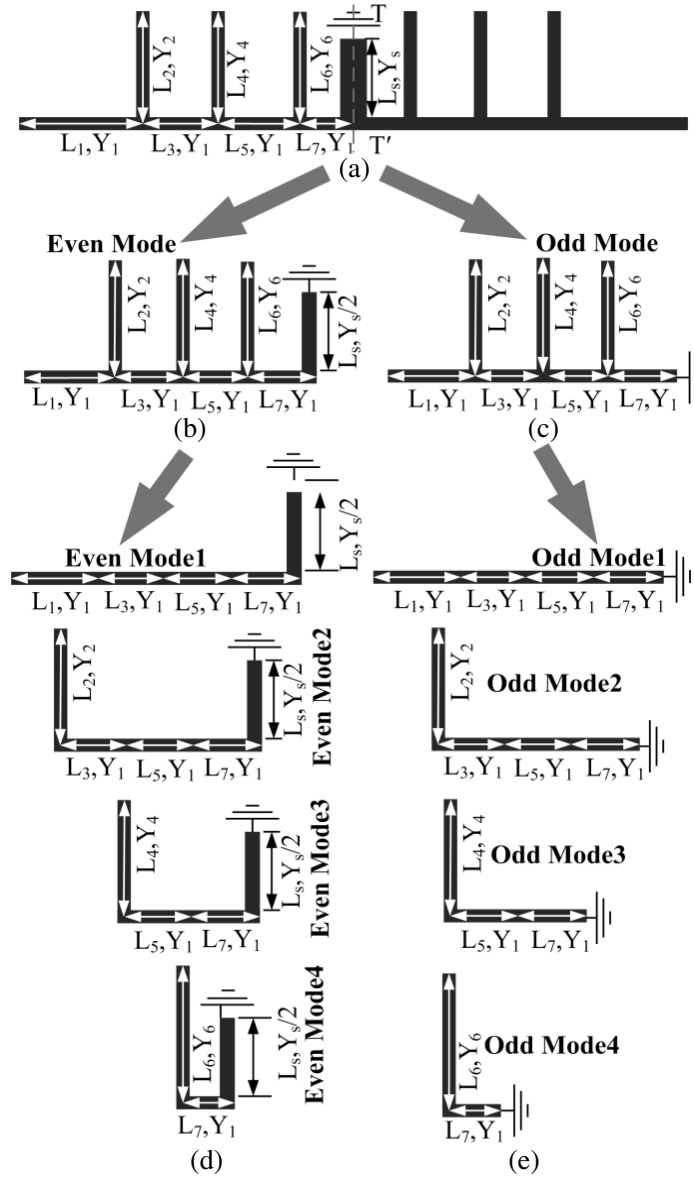
Figure 1. Even and odd mode decomposition of the proposed stub loaded resonator, (a) schematic diagram, (b) even-mode equivalent circuit, (c) odd-mode equivalent circuit, (d) decomposition of even-mode equivalent circuits of (b), (e) decomposition of odd-mode equivalent circuits of (c).

and

$$f_{\text{even4}} = \frac{(2n-1)c}{4\left(L_6 + L_7 + L_s\right)\sqrt{\varepsilon_e}} \tag{16}$$

In the above equations, "1"/"2"/"3"/"4" in the subscript of the LHS represents the band; Y_1, Y_2, Y_3, Y_4, Y_5, Y_6, Y_7 and Y_s represent the characteristic admittances of the respective line; L_1, L_2, L_3, L_4, L_5, L_6, L_7 and L_s represent the lengths of the respective line; $\theta_1 = \beta L_1$, $\theta_2 = \beta L_2$, $\theta_3 = \beta L_3$, $\theta_4 = \beta L_4$, $\theta_5 = \beta L_5$, $\theta_5 = \beta L_6$, $\theta_5 = \beta L_7$ and $\theta_s = \beta L_s$ represent the electric lengths of the respective lines; $n = 1, 2, 3, \ldots$, c represents the speed of light in free space; ε_e represents the effective dielectric constant of the substrate. In deriving the above resonance frequencies, we have assumed $Y_1 = Y_S/2$ for Equation (4), $Y_1 = Y_2$ for Equations (6) and (8), $Y_1 = Y_4$ for Equations (10) and (12), and $Y_1 = Y_6$ for Equations (14) and (16).
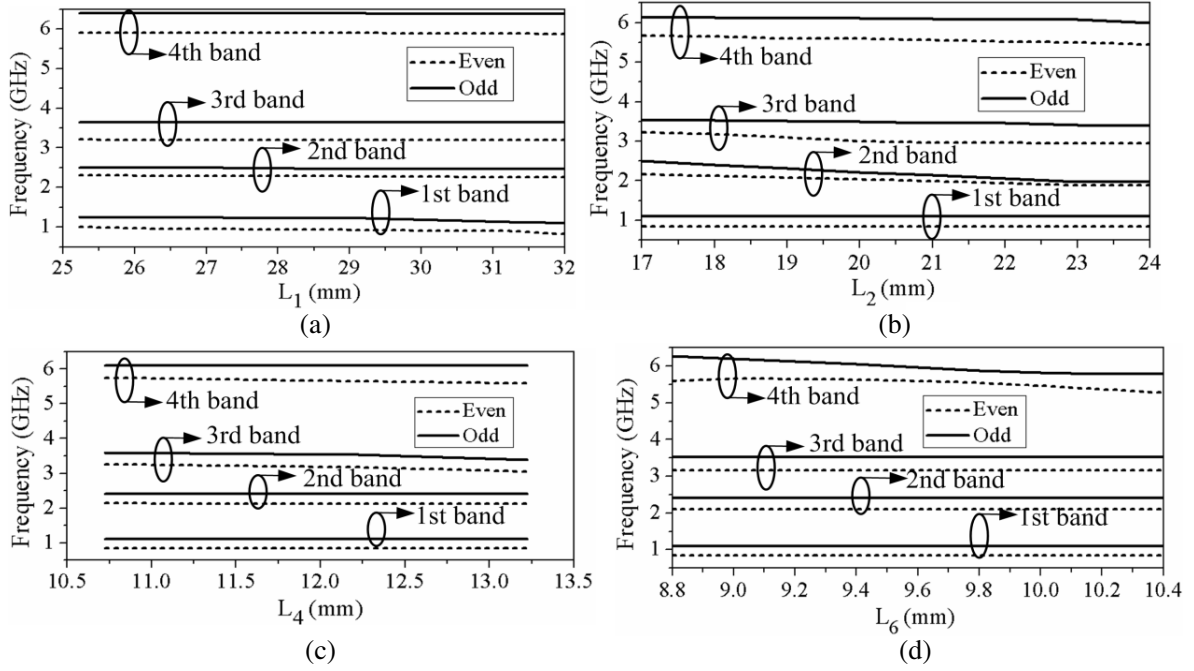
Figure 2. Simulated resonance frequencies of proposed SLR under weak coupling with different (a) L_1, (b) L_2, (c) L_4, and (d) L_6.

The pass bands of the quad-band BPF can be set by properly choosing the even and odd mode resonance frequencies, which can be set by a proper choice of the stub and resonator lengths. For example, according to the above analysis, f_{even1} and f_{odd1} determine the first pass band, and they can be set by a proper choice of the lengths L_1, L_3, L_5 and L_s. These lengths must satisfy Equations (2) and (4) as well as rest of the equations for given even and odd mode frequencies.

It may be noted that Equations (1)–(16) are valid for weak coupling or no coupling case. In the presence of strong coupling, the equations do not strictly hold, hence fine optimizations in the parameters are required. The effects of different parameters on the even/odd-mode resonance frequencies are shown in Figure 2. Optimizations are also required to account the coupling between the stubs at close proximity.

3. FILTER GEOMETRY

Figure 3 shows the layout of a quad-band BPF, which is designed based on the above analysis. The proposed quad-band BPF contains six open stubs at the two sides and a short-ended stub at the symmetrical plane of the resonator. The stub-loaded resonator has been tapped with a pair of $50\,\Omega$ microstrip transmission lines. The pass bands have been positioned by controlling individual stub lengths and stub widths. The open stubs are coupled with each other to minimize the circuit size and generate transmission zeros in the stopband. In this filter design, the four resonant frequencies are chosen as $0.9\,\text{GHz}$, $2.3\,\text{GHz}$, $3.5\,\text{GHz}$ and $5.8\,\text{GHz}$, respectively, corresponding to GSM, LTE 2300, $3.5\,\text{GHz}$ WiMAX and $5.8\,\text{GHz}$ WLAN applications. The filter is designed on a $0.762\,\text{mm}$ thick Rogers RO4350 substrate with a relative dielectric constant of 3.66 and loss tangent of 0.004.

Simulations are carried out using the 3D full-wave software ANSYS HFSS v14 in order to optimize the quad-band filter response. The optimized geometrical dimensions of the proposed filter are found as: $L_1 = 32.275$, $W_1 = 2$, $L_2 = 18$, $W_2 = 0.45$, $L_3 = 3.35$, $L_4 = 12.225$, $W_4 = 0.3$, $L_5 = 1.6$, $L_6 = 9.2$, $L_7 = 2.55$, $L_s = 2.5$, $L_g = 18$, $W_s = 0.5$, $g_1 = g_2 = g_3 = g_4 = 0.5$ and the grounding via diameter $= 0.5$ (all in mm).

The fabricated filter is shown in Figure 4. The total circuit area is $24 \times 20\,\text{mm}^2$ (or $0.13\lambda_g \times 0.1\lambda_g$, where λ_g corresponds to the guided wavelength at the center frequency of the lower passband), excluding the $50\,\Omega$ tapped transmission line.
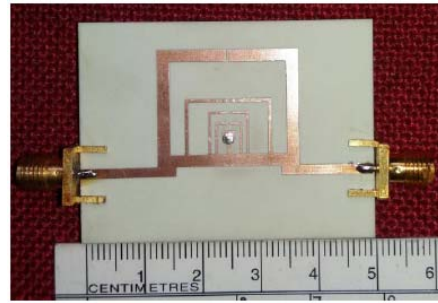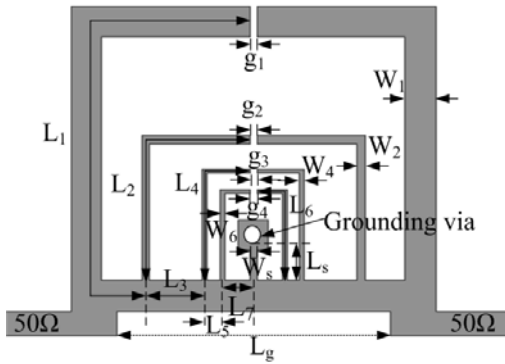
Figure 3. Layout of the proposed quad-band BPF.

Figure 4. Fabricated photograph of quad-band BPF.

4. RESULTS AND DISCUSSION

The frequency response of the proposed filter is shown in Figure 5, which reveals a reasonable agreement between the simulated and measured results over the operating frequency range. The measured passbands are located at 0.94, 2.27, 3.55 and 5.66 GHz, with 3 dB fractional bandwidths of 40.38%, 15.42%, 22.82% and 13.95%, respectively. The measured insertion losses (IL), including the losses from SMA connectors, in the four passbands are found to be 0.41, 2.06, 1.77, and 1.73 dB, respectively. Respective return losses are better than 18.3, 13.39, 12.8, and 13.9 dB. Eight transmission zeros, located at 1.46, 1.66, 2.73, 2.92, 4.13, 5.07, 6.18, and 6.67 GHz with more than 30 dB attenuations, insure better sharp band-to-band rejection. The TZs appear in the frequency response when the input admittance of the open stubs becomes infinity or the stubs become virtually grounded at the input. This corresponds to the condition

$$\cot \theta_Z = 0. \tag{17}$$

Under such a condition, the signal will be shorted to ground and cannot be transferred to the output port, which results in TZs. It can be shown that Equation (17) can be rewritten as [17]

$$f_Z = \frac{n\pi f_0}{2\theta_Z}, \quad n = 1, 3, 5 \tag{18}$$

where, f_o represents the desired resonant frequency. The bandwidths of each passband of the quad-band BPF filter can be controlled by W_1, W_2, W_4 and W_6 as shown in Figure 6 whereas passband return loss can be controlled by adjusting tapped position L_g, as shown in Figure 7.
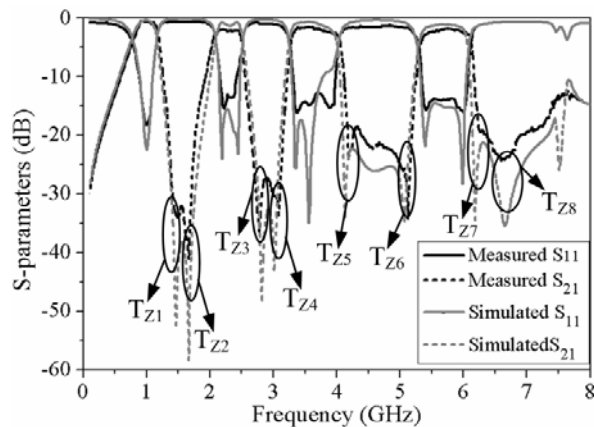
Figure 5. Simulated and measured frequency response of quad-band BPF.
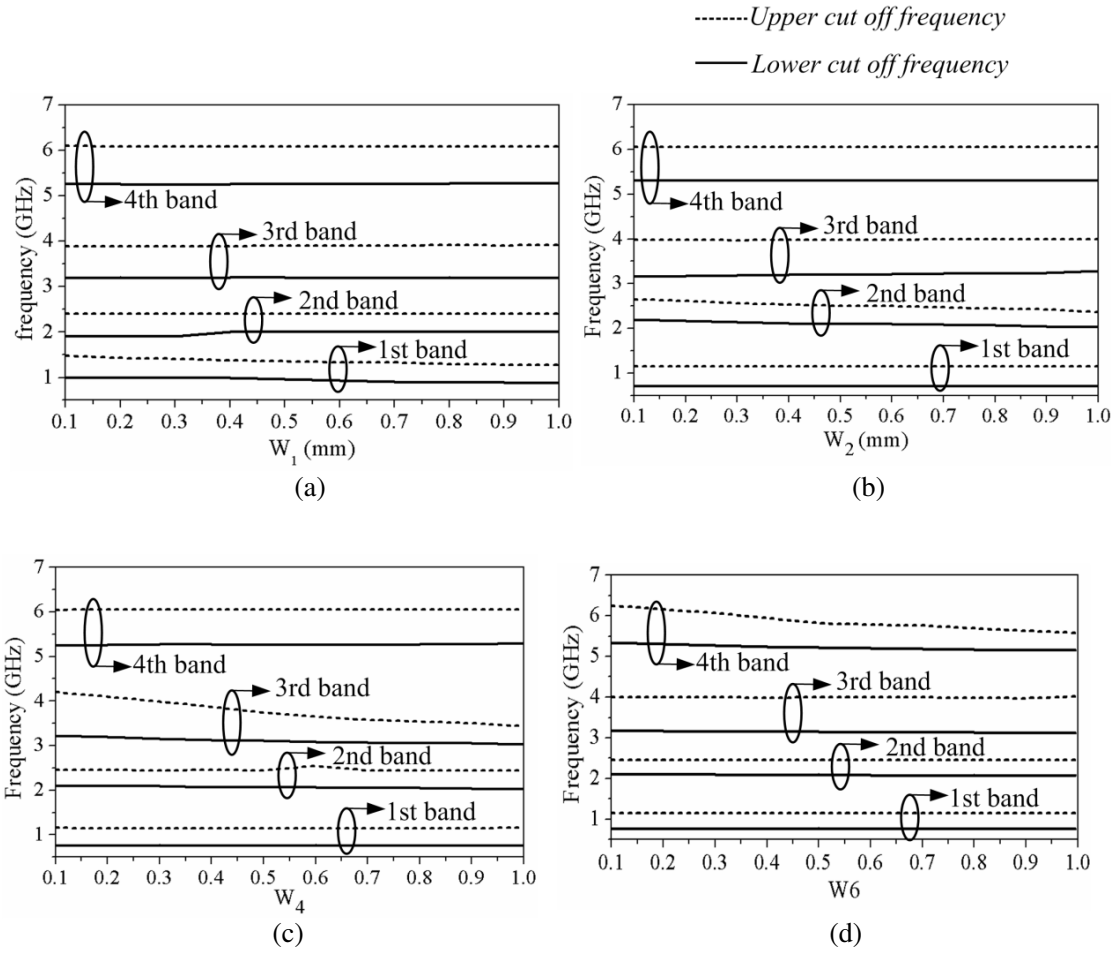
Figure 6. Simulated lower and upper cut-off frequencies of individual bands against various widths of proposed SLR, (a) W_1, (b) W_2, (c) W_4, and (d) W_6.
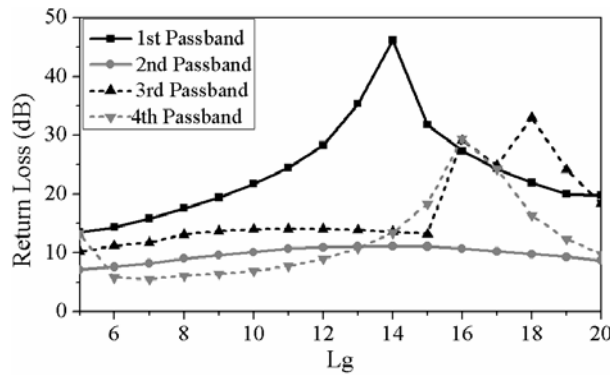
Figure 7. Variation of passband return loss with L_g.

Table 1 shows the comparison of the performance of the proposed quad-band filter with reported performance of some other quad-band BPFs. The table reveals that the proposed filter has realized miniaturization, high isolation, and low insertion loss.

Table 1. Comparison of the proposed filter with some past and presently reported quad-band BPFs.

Ref.	Frequency (GHz)	Circuit size ($\lambda_g \times \lambda_g$)	3 dB FBW (%)	IL (dB)
[9]	1.5/2.5/3.6/4.6	0.3 × 0.3	5.5/12/11/4.3	1.98/1.74/3.58/3.4
[10]	1.57/2.45/3.5/5.2	0.5 × 0.2	9.55/31.84/11.1/15.96	0.31/0.32/0.31/0.78
[15]	2.4/3.5/5.2/6.8	0.22 × 0.24	6.4/9.4/3.8/4.9	0.5/1.3/1.3/1.0
[16]	1.5/2.5/3.5/5.2	0.18 × 0.18	5.7/14.1/6.9/3.8	1.3/0.24/1.29/2.1
This work	**0.94/2.27/3.55/5.66**	**0.13 × 0.1**	**40.38/15.42/22.82/13.95**	**0.41/2.06/1.77/1.73**

5. CONCLUSION

In this paper, a miniaturized, multiband microstrip filter is presented that exhibits simultaneous operation at GSM, LTE, WiMAX, and WLAN bands. The multiband behaviour has been achieved due to loaded multiple stubs. The frequency response of the proposed filter shows low insertion loss, high return loss, and a very good sharp skirt. These features make the filter a good candidate for the modern wireless communication applications. Good agreements between the simulated and measured results are obtained, which validates the simulation.

REFERENCES

1. Zhang, X. Y., J.-X. Chen, and Q. Xue, "Dual-band bandpass filters using stub-loaded resonators," *IEEE Microwave and Wireless Components Letters*, Vol. 17, No. 8, 583–585, August 2007.

2. Lai, X., C.-H. Liang, H. Di, and B. Wu, "Design of tri-band filter based on stub loaded resonator and DGS resonator," *IEEE Microwave and Wireless Compon Letters*, Vol. 20, No. 5, 265–267, May 2010.

3. Lan, S. W., M. H. Weng, and S. J. Chang, "A tri-band bandpass filter with wide stopband using asymmetric stub-loaded resonators," *IEEE Microwave and Wireless Components Letters*, Vol. 25, No. 1, 19–21, January 2015.

4. Wei, F., Y. J. Guo, P.-Y. Qin, and X. W. Shi, "Compact balanced dual- and tri-band bandpass filters based on stub loaded resonators," *IEEE Microwave and Wireless Components Letters*, Vol. 25, No. 2, 76–78, February 2015.

5. Murmu, L. and S. Das, "A dual-band bandpass filter for 2.4 GHz bluetooth and 5.2 GHz WLAN applications," *Progress In Electromagnetics Research Letters*, Vol. 53, 65–70, 2015.

6. Quendo, C., A. Manchec, Y. Clavet, E. Rius, J.-F. Favennec, and C. Person, "General synthesis of N-band resonator based on norder dual behavior resonator," *IEEE Microwave and Wireless Components Letters*, Vol. 17, No. 5, 337–339, May 2007.

7. Zhang, Y., K. A. Zaki, J. A. Ruiz-Cruz, and A. E. Atia, "Analytical synthesis of generalized multi-band microwave filters," *IEEE MTT-S Int. Microwave Symp. Dig.*, 1273–1276, June 2007.

8. Hejazi, Z. M., "A fast design approach of compact microstrip multiband bandpass filters," *Microwave and Optical Technology Letters*, Vol. 54, No. 4, 1075–1079, April 2012.

9. Wu, J. Y. and W. H. Tu, "Design of quad-band bandpass filter with multiple transmission zeros," *Electronics Letters*, Vol. 47, No. 8, 502–503, April 2011.

10. Cheng, C.-M. and C.-F. Yang, " Develop quad-band (1.57/2.45/3.5/5.2 GHz) bandpass filters on the ceramic substrate," *IEEE Microwave and Wireless Components Letters*, Vol. 20, No. 5, 268–270, May 2010.

11. Cho, Y. H. and S. W. Yun, "A tri-band bandpass filter using stub-loaded SIRs with controllable bandwidths," *Microwave and Optical Technology Letters*, Vol. 56, No. 12, 2907–2910, December 2014.

12. Mo, Y., K. Song, and Y. Fan, "Miniaturized triple-band bandpass filter using coupled lines and grounded stepped impedance resonators," *IEEE Microwave and Wireless Components Letters*, Vol. 24, No. 5, 333–335, May 2014.

13. Ching-Her, L., C. I. G. Hsu, and H. Chih-Chan, "Balanced dual-band BPF with stub-loaded SIRs for common-mode suppression," *IEEE Microwave and Wireless Components Letters*, Vol. 20, No. 2, 70–72, February 2010.

14. Jin, S. and X. Quan, "Novel balanced dual-band bandpass filter using coupled stepped-impedance resonators," *IEEE Microwave and Wireless Components Letters*, Vol. 20, No. 1, 19–21, January 2010.

15. Wei, W. H. and Y. R. Yuan, "A new quadband bandpass filter using asymmetric stepped impedance resonators," *IEEE Microwave and Wireless Components Letters*, Vol. 21, No. 4, 203–205, April 2011.

16. Wei, F., Q. L. Huang, W.-T. Li, and X.-W. Shi, "A compact quadband bandpass filter using novel stub loaded SIR structure," *Microwave and Optical Technology Letters*, Vol. 56, No. 3, 538–542, March 2014.

17. Xu, J., W. Wu, and C. Miao, "Compact microstrip dual-/tri-/quad-band bandpass filter using open stubs loaded shorted stepped-impedance resonator," *IEEE Transactions on Microwave Theory and Techniques*, Vol. 61, No. 9, 3187–3199, September 2013.